Nanomed Res J 5(2):120-131, Spring 2020

RESEARCH ARTICLE

Preparation, statistical optimization and in vitro characterization of solid lipid nanoparticles as a potential vehicle for transdermal delivery of tramadol hydrochloride as a hydrophilic Compound

Mina Abbasnia[1], AlirezaVatanara[2], Reza Mahjub[1*]

[1]Department of Pharmaceutics, Faculty of pharmacy, Hamedan University of Medical Science, Hamedan, Iran

[2]Department of Pharmaceutics, Faculty of Pharmacy, Tehran University of Medical Science, Tehran, Iran

ARTICLE INFO

Article History:
Received 11 February 2020
Accepted 06 April 2020
Published 15 May 2020

Keywords:
Tramadol Hydrochloride
Hydrophilic drug
Solid lipid nanoparticles (SLN)
Double emulsification-Solvent evaporation technique
Central-composite response surface methodology
Transdermal delivery

ABSTRACT

As encapsulation of hydrophilic drugs in the solid lipid nanoparticles (SLNs) is still a challenging issue, the aim of this study was to prepare SLNs containing tramadol hydrochloride as a hydrophilic compound. The SLNs were prepared using glycerol monostearate (GMS), soy lecithin and tween 80 by double emulsification-solvent evaporation technique. The nanoparticles were optimized through a central-composite response surface (RSM) method. The independent variables were GMS/lecithin ratio and the amount of drug while dependent responses were size, poly dispersity index (PdI) and zeta potential. The optimized nanoparticles were then freeze dried and their morphology was examined using transmission electron microscopy (TEM). Finally, the in vitro drug release profile from nanoparticles was evaluated and the kinetic of the release was determined. The particle size, PdI, zeta potential, entrapment efficiency and loading efficiency of the optimized SLNs were 131±17.25 nm, 0.21±0.013, -11.2 ±1.04 mV, 89.4±2.38% and 9.49±0.14%, respectively. TEM images revealed de-agglomerated spherical nanoparticles. In vitro release studies showed sustained release of tramadol over 72 h. The release kinetic was best fitted to the first order and Korsmeyer-Peppas kinetic model. The obtained results indicated that tramadol as a hydrophilic compound can entrap appropriately in the solid lipid nanoparticles exhibiting favorable physico-chemical properties.

How to cite this article
Abbasnia M, Vatanara AR, Mahjub R. Preparation, statistical optimization and in vitro characterization of solid lipid nanoparticles as a potential vehicle for transdermal delivery of tramadol hydrochloride as a hydrophilic Compound. Nanomed Res J, 2020; 5(2): 120-131. DOI: 10.22034/nmrj.2020.02.003

INTRODUCTION

Tramadol hydrochloride is a synthetic analgesic bearing aminocyclohexanol chemical structure, which is mostly used in post-operational pain managements as well as controlling cancer-induced pains by both opioid and non-opioid mechanisms of action. The analgesic effects of tramadol are approximately 10-times greater than morphine which makes the compound as a good candidate for pain reduction. The non-opioid mechanism of tramadol is believed to be through the agonistic features in serotonergic and dopaminergic receptors along with prevention of their re-uptake, while the opioid mechanism is through stimulation of μ receptors [1]. Shortly after oral administration, the active metabolite of O –desmethyl tramadol, known as M_1, which is a strong μ agonist and responsible for addiction features, is produced as the result of the first pass metabolism (FPM) of the parent drug in the liver [2]. The chemical structure of the tramadol and the active metabolite M_1 are shown in (Fig.1). Although the compound exhibits less adverse effects than other opioids, the short plasma half-life (i.e. 4-6 hrs) and the potential for drug addiction are count as the major drawbacks

* Corresponding Author Email: *r.mahjoub@umsha.ac.ir*

This work is licensed under the Creative Commons Attribution 4.0 International License.
To view a copy of this license, visit http://creativecommons.org/licenses/by/4.0/.

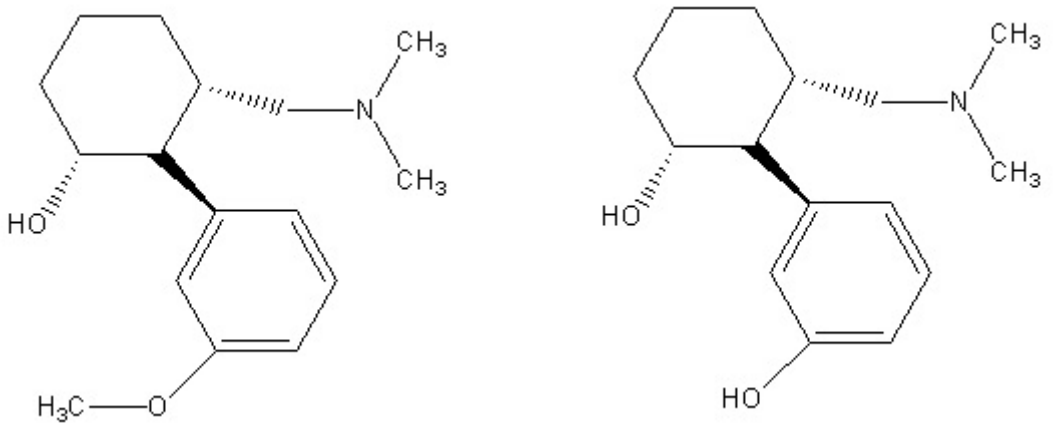

Fig.1. Chemical structures of A) Tramadol; B) O-desmethyl-tramadol (M_1)

of tramadol. Therefore, preparation of a non-oral, sustained-release formulation which can bypass FPM effect will promote therapeutic efficacy and reduce addictive potential of tramadol [3].

Solid lipid nanoparticles (SLNs) are introduced in 1990 as a replacement for emulsions, liposomes and polymeric nanoparticles and because of their ease of manufacturing, improved stability and their high biocompatibility, these nanoparticles are highly investigated [4]. These nano-structures are designated as spherical particles with 10-1000 nm in diameter containing a lipophilic matrix-like core which is stabilized using surfactants [5, 6] and can incorporate both hydrophilic and lipophilic therapeutic compounds [7]. These nanoparticles have the potential to be easily incorporated in transdermal patches for improving the efficiency in transdermal delivery of tramadol [8, 9].

While numerous methods have been successfully developed for incorporation of lipid-soluble compounds into SLNs, preparation of formulations containing lipid-insoluble drugs is more challenging. During fabrication of SLNs, drugs with poor lipid solubility are intrinsically expelled from the lipid matrix into the dispersing aqueous phase. The double emulsification-solvent evaporation (DESE) method in which, by producing a $W_1/O/W_2$ double emulsion, W_1 can encapsulate the compounds which exhibit high aqueous solubility and the oil phase plays the role of a diffusion barrier for prevention of drug transport from W_1 to W_2 phases [10, 11]. In this study, tramadol-loaded SLNs were prepared using DESE and a central-composite experimental design was employed in order to produce formulations bearing optimized physico-chemical characteristics.

MATERIALS AND METHODS

Materials

Glyceryl monostearate (GMS) was purchased from Sigma™ (St. Louis, MO, USA), Soy lecithin (SL), tween 80 and sucrose were supplied by Samchun™ (Seoul, South Korea). Sodium chloride, potassium chloride, disodium hydrogen phosphate (Na_2HPO_4), potassium dihydrogen phosphate (KH_2PO_4) and analytical grade acetonitrile were obtained from Merck™ (Darmstadt, Germany). Tramadol hydrochloride was provided from Zhengzhu Debo™ (China). Analytical grade water was provided using Milipore® water purification system.

Preparation of solid lipid nanoparticles encapsulating tramadol hydrochloride

Tramadol hydrochloride-loaded SLNs were prepared by DESE method [4]. Briefly, various amounts of GMS and soy lecithin (50 mg) were dissolved in 5 ml dichloromethane (organic phase). The first aqueous phase (W_1) was prepared by dissolving different amounts of tramadol hydrochloride in 2 ml of de-ionized water which was previously filtered through 0.22 µm syringe filter. The first aqueous (W_1) phase was then emulsified into the organic phase using a homogenizer at 20,000 rpm for 10 min. Then after, the prepared W /O emulsion was added using a syringe pump at[1]a rate of 2 ml/min into 25 ml of aqueous tween 80 (1% w/v) solution (W_2) under

CC BY

high-speed homogenization (20,000 rpm) and kept homogenizing for a period of 15 minutes. In order to remove the organic solvent, the prepared emulsion was evaporated by a Heidolph™ (Germany) rotary evaporator to produce SLNs. The nanoparticles were then settled down by centrifugation at 20,000 rpm using a Beckman-Coulter Optima™ XPN-100 ultracentrifuge (Georgia, United States) for 30 min at 4 °C, and washed twice with de-ionized water. The retrieved nanoparticles were then re-suspended in 3 ml of 5 % (w/v) sucrose and frozen at -20 °C before final lyophilization at -40 °C for 48 h.

Quantification of tramadol by reversed phase liquid chromatography

Tramadol HCl was quantified by previously reported RP- HPLC method [12] using Shimadzu™ LC-20AD HPLC system (Kyoto, Japan) equipped with SPD-10A vp UV-Visible detector that was set at the wavelength of 270 nm. Shimadzu ODS C18 column (250 mm × 4.6 mm) was applied as the solid stationary phase. The mobile phase was consisted of water and acetonitrile (10:90). The pump flow was set at 0.5 ml min^{-1}. The peaks were automatically integrated using lab solution® software. The method represented a good linearity between 1 and 100 µg/ml with a regression coefficient (R^2) of 0.9991. The limit of detection (LOD) and limit of quantification (OQ) were determined by signal to noise ratio and were reported as 0.11 µg/ml and 0.9 µg/ml, respectively. De-ionized water was used as the solvent for preparation of working standards of tramadol HCl.

Characterization of Nanoparticles

The mean particle size (Z-average) and poly dispersity index (PdI) of nanoparticles were determined by dynamic light scattering (DLS) using a Malvern® zetasizer- nanosizer (Malvern® instruments, United Kingdom). Zeta potential of nanoparticles was evaluated by the same instrument using electrophoretic mobility of nanoparticles using Smoluchowski's equation.

The percentage of EE % and LE % were indirectly calculated by determination of the drug content in the clear supernatant which was obtained after centrifugation of freshly prepared colloidal nano-suspension. Analysis of the free drug content in the supernatant was performed by HPLC. Thenafter, EE% and LE% were calculated by reduction of un-entrapped drugs from total drug contents using following equations :

$$Entrapment\ Efficinecy\left(EE\%\right) = \frac{\left(Mass\ of\ initial\ drug - Mass\ of\ free\ drug\right)}{Mass\ of\ initial\ drug} * 100 \quad (1)$$

$$Loading\ Efficiency\left(LE\%\right) = \frac{\left(Mass\ of\ initial\ drug - Mass\ of\ free\ drug\right)}{Weight\ of\ Nanoparticles} * 100 \quad (2)$$

Experimental design studies

The central-composite design experiments were carried out in 13 sets with different values of independent variables. According to the fractional factorial experimental design that was previously performed as the preliminary study (data was not shown), the amount of tween 80 and soy lecithin were kept constant at 1% w/v and 50 mg, whereas the ratio of GMS to soy lecithin as well as the amount of drug were varied. The range and constrains of independent variables, determined by the preliminary study, are summarized in (Table 1). Different experimental runs with various compositions as F_1 to F_{13} were designed (Table 2) and were experimentally prepared. All the measurements were performed in triplicate. All

Table 1. Ranges and constrains of variables used in experimental design.

Independent variables (Factors)		Levels	
		-1	+1
Numeric factors	GMS/ soy lecithin concentration ratio (X_1)	0.2	1.0
	Amount of drug (mg) (X_2)	10	30
Dependent variables (Responses)	**Constrains**		
Y_1=Size (nm)	Minimize		
Y_2=PdI	Minimize		
Y_3=Zeta Potential (mV)	-20 < Zeta < -10		

(cc) BY

Table 2. Central composite experimental design (n=3).

No.	Independent variables		Dependent variables		
	GMS/ soy lecithin (X_1)	B: Drug (mg) (X_2)	Size (nm) (Y_1) Mean±SD	PdI (Y_2) Mean±SD	Zeta potential (mV) (Y_3) Mean±SD
F_1	1.00	30.00	352±32	0.899±0.001	-22.70±2.52
F_2	0.20	30.00	253±27	0.562±0.003	-5.40±0.37
F_3	0.60	5.86	1075±19.8	0.285±0.003	-16.40±1.48
F_4	0.60	20.00	257±15.9	0.642±0.004	-14.60±1.21
F_5	0.60	20.00	235±26.5	0.571±0.001	-13.80±0.65
F_6	0.60	20.00	241±20.5	0.604±0.002	-14.10±0.20
F_7	0.03	20.00	143±26.7	0.145±0.002	-3.70±0.61
F_8	0.60	20.00	252±24.7	0.657±0.001	-14.70±1.21
F_9	0.20	10.00	371±24.6	0.326±0.002	-10.50±2.62
F_{10}	1.00	10.00	843±25.9	0.242±0.005	-34.25±4.33
F_{11}	1.17	20.00	677±14.61	0.375±0.002	-31.10±2.50
F_{12}	0.60	34.14	344±12.4	0.867±0.001	-12.10±0.42
F_{13}	0.60	20.00	237±24.6	0.631±0.003	-13.90±0.21

results were analyzed statistically using design-expert®.

In model fitting analysis, experimental data including particle size (Y_1) , PdI (Y_2) and zeta potential (Y_3) were treated by the software and the best appropriate mathematical model was determined for each response. The significancy level was set at *0.05*. Co-efficient of each significant effect was further used to develop a reduced equation by step-wise multiple regression analysis. The interactions between independent variables were visually explained by using 3-D response surface plots.

In order to validate the proposed models and evaluation of prediction errors, the suggested optimized formulation was prepared experimentally in five times and characterized by determination of their particle size, poly dispersity index (PdI), zeta potential (mV), entrapment efficiency (EE%) and loading efficiency (LE%). The predicated error% was calculated based on the following equation (Eq.3):

$$Prediction\ error\% = \frac{(Observed\ response - Predicted\ response)}{Observed\ response} * 100 \quad \textbf{(3)}$$

Freeze drying of nanoparticles

Freeze drying of SLNs was performed on experimentally prepared optimized formulation of nanoparticles. Before freeze-drying process, the settled down optimized nanoparticles were reconstituted by sucrose 5% (w/v) as the lyo-protectant. Then, the re-dispersed colloidal suspension was freeze-dried using Operon™ freeze dryer (FDB 5503, Korea). After freeze drying, the lyophilized SLNs were reconstituted in mili-Q water for re-evaluation of parameters including particle size, PdI and zeta potential. The effects of the lyophilization process on physico-chemical characteristics of nanoparticles were also studied by comparing the characteristics of nanoparticles before and after lyophilization using two sample independent t-test which was performed by SPSS® software (V16.0.0).

Determination of the morphology of the particles

Lyophilized nanoparticles were morphologically examined by transmission electron microscopy (TEM) which was performed by a Zeiss EM10C 100kV (Germany). Before the experiment, samples were coated with holey carbon coated grid Cu Mesh 300.

In Vitro release studies

The release profile of tramadol from the colloidal suspension was studied *in vitro* by using a dialysis bag under sink condition. Phosphate buffered saline adjusted to pH of 7.4 was used as the release medium [13]. Proper amounts from tramadol-containing SLNs colloidal suspension equivalent to 2.5 mg of tramadol hydrochloride was placed in a dialysis bag (MWCO 12 KDa) and was subsequently

CC BY

Table 3. Characteristics of the best fitted mathematical models.

Dependent variables (responses)	Best fitted model	Adeq percision	Pred R-squared	Adj R-squared	R-squared
Size (Y_1)	Quadratic	15.741	0.7024	0.8864	0.9243
PdI(Y_2)	Quadratic	22.288	0.8516	0.9499	0.9666
Zeta Potential (Y_3)	Quadratic	24.19	0.8807	0.9432	0.9574

immersed in 200 ml of the pre- heated phosphate buffer, maintained at 37±2°C while stirring at 100 rpm. At predetermined times; one mililiter of the medium was collected and simultaneously replaced by the same amount of freshly prepared pre-heated buffer. The concentration of tarmadol in the collected samples was quantified using HPLC equipped with UV detector that was set at 270 nm.

For determination of the release kinetic, the data were fitted to various release kinetic models including zero order, first order, higuchi, korsmeyer-peppas and hixon- crowell models and their appropriate correlation coefficients were investigated using Sigma-plot® software (version 10.0.0.54)[14].

Statistical analysis

In this study, all experiments were performed in triplicate except otherwise stated which were carried out experimentally in five times. Comparison of two groups of data performed using two sample independent t-test by SPSS® software (V.16.0). Central- composite experimental design and model fitting were accomplished by design expert® software (V.7.0.0).

RESULTS AND DISCUSSION

Preparation and characterization of solid lipid nanoparticles

In this study, central-composite design was employed for preparation of statistically optimized solid lipid nanoparticles and evaluation of the effects of all main factors and possible their binary interactions on pre-determined responses. Therefore, a set of 13 formulations from tramadol-loaded SLNs were experimentally fabricated. The values of independent variables and the related experimentally obtained responses in the various formulations (i.e. F_1-F_{13}) are illustrated in (Table 2).

In this study, analysis of responses using design-expert™ software, showed that all dependent variables including particle size (Y_1), PdI (Y_2) and zeta potential (Y_3) were fitted to quadratic models with the significant model p values (p *<0.0002*). The statistical and mathematical characteristics of the proposed models are summarized in (Table 3).

Size of the particles

The obtained values for particle size with mean diameter ranging from 235±26.5 nm (i.e. formulation F_5) to 1075±19.8 nm (i.e. formulation F_3) are shown in (Table 2). For prediction of particle sizes, statistical analysis performed by the software was applied to establish the proper significant fitted model. Characteristics of the fitted model are summarized in (Table 3). Analysis of variance for data revealed that the linear coefficients of all independent factors as well as the squared coefficient of the amount of drug (X_2^2) were significant (p*< 0.001*). However, no significant binary interaction was found between the two independent variables (p*>0.05*).The coefficients of significant variables on particle size (Y_1) are shown in Eq. 4 as follows:

$$Y_1 = + 283.74 + (165.77*X_1) - (205.35*X_2) - (93.25*X_1.X_2) + (198.92*X_2^2) \quad \textbf{(4)}$$

Where:

Y_1: particle size;

X_1: Coefficient for GMS/ Lecithin ratio;

X_2: Coefficient for the amount of drug;

X_2^2: Squared coefficient for the amount of drug

$X_1.X_2$: Binary interaction coefficient;

As shown in the equation and illustrated in the 3D response surface plot (Fig.2(a)), it is observed that by increasing the ratio of GMS/ lecithin (X_1), the values for particle size would raised dramatically. Moreover, in the preliminary fractional factorial experimental design study (data not shown), it was showed that by increasing GMS/lecithin ratio to 5.0, the size of particles were risen to over 7,000 nm. Glyceryl monostearate, as the central core, forms the lipid matrix of the SLNs. Therefore, it is sensible that in higher ratios of GMS/lecithin, an increased particle size could be observed [15]. This phenomenon was in well accordance with previous studies which showed the dependency of the size

(cc) BY

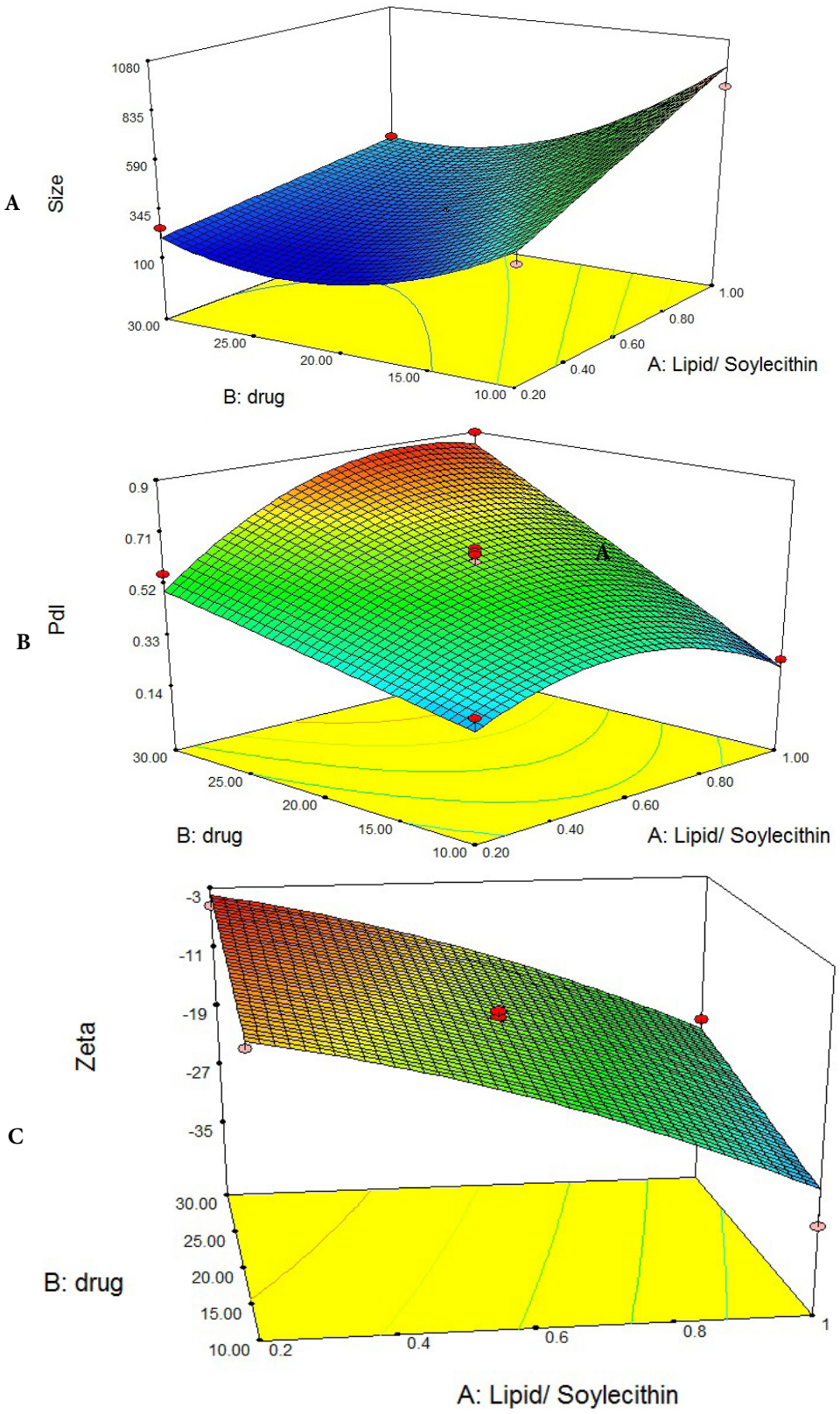

Fig.2. 3D response surface plots for bionary interactions on A) Size of particles; B) Poly dispersity index and C) Zeta potential;

CC BY

of SLNs on the amount of GMS as the lipid matrix and it was reported that in high concentration of GMS, the larger particles would be obtained due to coalesce of the lipid matrix [16]. According to Stoke's law, it can be justified by considering the difference in densities between internal and external phase of the prepared emulsion. Moreover, the study of Mehnert and Mader [17] demonstrated that particle size of SLNs would be increased by increasing the lipid content of the nanoparticles. This can be due to an increase in viscosity of the inner phase and therefore reduction in homogenization efficiency as the result of increasing the amount of the lipid [15, 18]. Moreover, it was showed that, in lower amounts of lipids, the ability of surfactants in stabilizing the particles was enhanced and therefore smaller particles were obtained [19].

On the other hand, as shown in Fig.2a, although size of particles were dramatically declined by rising the amount of drug from 10 miligram to approximately 20 miligram, but by further increase in drug concentration up to 30 mg, the particle size of SLNs were slightly decreased.

Polydispersity index (PdI)

The homogeneity of nano-suspensions becomes higher as the PdI approaches to zero (Mahjub R et al. 2016). As shown in (Table 2), the experimentally observed PdI is ranged from 0.145±0.002 (i.e. formulation F_7) to 0.899 ± 0.001 (i.e. formulation F_1). For prediction of PdI values, statistical analysis performed by the software was applied to establish the proper significant fitted model. Characteristics of the fitted model are summarized in (Table 3). Analysis of variance for data revealed that the linear coefficients of all independent factors, squared coefficient of GMS/lecithin (X_1^2) as well as the binary interaction between two independent factors ($X_1.X_2$) were significant ($p<0.004$). The coefficients of significant variables on pdI (Y_2) are shown in Eq. 5 as follows:

$$Y_2 = +0.62+(0.072*X_1)+(0.21*X_2) +(0.11*X_1.X_2)-(0.16*X_1^2) \quad \textbf{(5)}$$

In which:

Y_2: Polydispersity index of nanoparticles;

X_1: Coefficient for GMS/ Lecithin concentration ratio;

X_2: Coefficient forthe amount of drug;

$X_1.X_2$: Coefficient for binary interaction;

X_1^2: Squared coefficient for GMS/Lecithin ratio;

As it is demonstrated in the 3D response surface plot (Fig.2(b)), in highest GMS/lecithin ratio (i.e. 1.0), the poly dispesity index increased dramatically followed by rising the amount of the drug from 10 mg to 30 mg. However, in the lowest GMS/lecithin ratio (i.e. 0.2), increasing the amount of drug would resulted in slight increase in PdI. On the other hand, in either lowest or highest amount of drug, raising the GMS/lecithin ratio from 0.2 to 0.6 could result in the slight rise in PdI. However, by further increase in the ratio, the PdI values were fall dramatically.

Zeta potential

As shown in (Table 2), the experimentally observed zeta potential is varying between -34.25±4.33 mV (i.e. formulation F_{10}) and -3.70±0.61 mV (i.e. formulation F_7). For prediction of zeta potentials, statistical analysis performed by the software was applied to establish the proper significant model. Characteristics of the fitted model are summarized in (Table 3). Analysis of variance for data revealed that while linear coefficients of all independent factors and squared-coefficient of GMS/lecithin (X_1^2) were significant ($p<0.004$), the binary interaction between two independent variables was not considered significant ($p>0.1$). The coefficients of significant variables on zeta potential (Y_3) are shown in Eq. 6 as follows:

$$Y_3= -10.106 – (9.134* X_1) + (0.284* X_2) – (13.169* X_1^2) \quad \textbf{(6)}$$

Where:

Y_3: Zeta potential of nanoparticles;

X_1: Coefficient for GMS/ Lecithin concentration ratio;

X_2: Coefficient for the amount of drug;

X_1^2: Squared coefficient for GMS/ Lecithin ratio;

As it is illustrated in the 3D response surface plot (Fig.2(c)), zeta potentials were dramatically declined by increasing the ratio of GMS/ soy lecithin. It is suggested that as the result of increasing the concentration of the lipid, the surface accumulation of the GMS, which impose negative charges, would increase and therefore it is expected that zeta potential of the particles become more negative in higher GMS/ lecithin ratios.

On the other hand, it is shown in the figure that by raising the amount of drug, the zeta potential of the particles was slightly increased. Considering the chemical structure of tramadol (Fig.1 (a)), the compound bearing positive charge due to ionization

(cc) BY

Table 4. Optimized independent variables and predicted responses.

No.	Optimized independent Variables		Predicted dependent Variables (Responses)			Desirability
	Lipid/lecithin(X_1)	Drug(X_2)	Y_1=Size(nm)	Y_2=PdI	Y_3=Zeta	
1	0.27	12.62	148.88	0.226	-12.0	0.744

Table 5. The observed responses for predicted optimized formulations (n=5).

Size (nm)		Zeta Potential (mV)		PdI		EE%	LE (%)
Observed response (Mean±SD)	Prediction Error (%)	Observed response (Mean±SD)	Prediction Error (%)	Observed response (Mean±SD)	Prediction Error (%)	Observed response (Mean±SD)	Observed Responses (Mean±SD)
131±17.25	-9.83%	-11.2±1.04	-7.14%	0.210±0.013	-7.61%	89.4±2.38	9.49±0.14

of primary amine groups. Although the drug was suggested to mainly incorporate in the inner aqueous phase but in high amounts of drug, surface accumulation of some tramadol molecules is also proposed. Therefore, by increasing the amount of drug, zeta potential of the particles were observed to increase as the result of surface incorporation of the positively charged tramadol.

Optimization and model validation

The optimization of the physico-chemical characteristics of SLNs was carried out according to statistical and mathematical modeling of experimental data using central-composite response surface methodology. The optimized and predicted parameters for preparation of SLNs are shown in (Table 4). To determine the model validation and calculation of the appropriate prediction errors, the suggested optimized formulation were prepared and characterized experimentally ($n=5$). The observed responses and the values of predicated errors are indicated in (Table 5). As shown in the table, the calculated prediction errors were below 10% for all responses demonstrating the proper predictability, efficiency and adequacy of the proposed models.

Size, Entrapment efficiency (EE %), drug loading (DL %) and zeta potential are considered as the most important physico-chemical characteristics of colloidal systems. Accordingly, size of optimized nanoparticles was determined as 131±17.25 nm with high degree of hemogenicity. EE% of optimized SLN formulation was calculated and determined as high as 89.4±2.38% (Table 5) which indicates that tramadol HCl can be successfully encapsulated into the nanostructures with high efficiency. In any drug delivery systems, it is favor to achieve the highest EE%. Higher values for EE% indicate higher payload of the therapeutic agents into the particulate carrier and therefore can render the system more efficient in producing more therapeutic outcome. Due to the importance of EE% in development of a drug carrier, Malekpour et al. [20] applied artificial neural network (ANN) methodology to predict and optimize the entrapment efficiency in mPEG-PLGA nanoparticles encapsulation curcumin as a therapeutic agent. Furthermore, Shahsavari et al. [21] investigated the application of ANN in optimization of size, PdI, zeta potential and EE% of the insulin nanoparticles composed of quaternized derivatives of chitosan. Loading efficiency (LE %) is also an effective parameter in characterization of nanoparticles and in this study, it is reported to be 9.49±0.14% (Table 5). Zeta potential of the particles is considered as the well indicator for prediction of the stability of the colloidal dispersion [22]. Accordingly, particle aggregation is less likely to occur in high zeta potentials (either positive or negative) due to significant electrostatic repulsion force between particles [23]. Therefore, nanoparticles with zeta potential values above +10 mV or below 10 mV exhibit high stability [24]. As shown in (Table 5), zeta potential of the optimized SLNs was determined as -10.8±1.04 mV which can ensure proper stability for the tramadol HCl loaded SLNs. According to the previous studies, the negative charge of zeta potential is related to surface accumulation of negatively charged lipids in solid lipid nanoparticles [25, 26].

CC BY

Table 6. Physico-chemical characteristics of nanoparticles (after lyophilization; n=3).

Characteristics	After lyophilization
Particle size	186±26.31 nm
PdI	0.22±0.018
Zeta potential	-3.7±1.98 mV

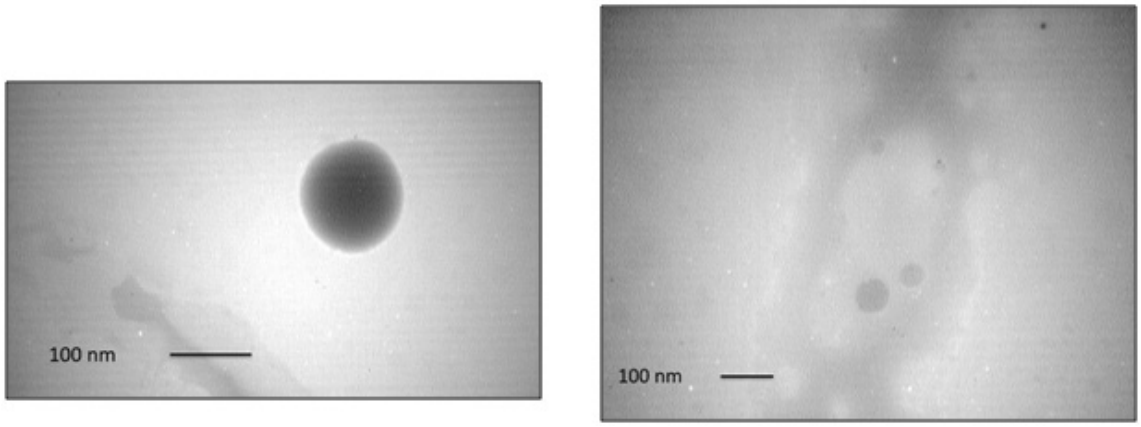

Fig.3. TEM images of Nanoparticles;

Lyophilization of nanoparticles

The impact of lyophilization process on characteristics of the solid lipid nanoparticles including particle size, PdI and zeta potential was investigated and the appropriate results are illustrated in (Table 6). Previous studies revealed that di-saccharide sugars such as sucrose are more efficient cryo-protectant compared to mono-saccharide counterparts such as mannitol, sorbitol and terhalose and consequently exhibit higher efficiency in conserving the physico-chemical features of nanoparticles during lyophilization[27].

As shown in (Table 6), the size of nanoparticles was significantly increased from 131±17.25nm to 186± 26.31 nm ($p < 0.05$), during lyophilization. On the other hand, while PdI of particles was not significantly changed ($p>0.05$) as the result of freeze drying, the zeta potential of the particles were significantly increased from -11.2±1.04 mV to -3.7±1.98 mV. Determination of zeta potential is an effective method to consider the eventual interactions between the cryo-protectant molecules and the surface of nanoparticles [28, 29]. The significant reduction in negative surface charge can be justified by considering the surface accumulation of sucrose as lyoprotectant and therefore masking the negative charges of lipids [30, 31].

Morphological studies

Images obtained from transmission electron microscopy of optimized SLN preparation are illustrated in (Fig. 3). As shown in the figure, TEM images revealed formation of non-aggregated, spherical shaped solid lipid nanoparticles and their approporiate diameters were in well accordance with data obtained by photon correlation spectroscopy (PCS).

In vitro release study

The *in vitro* release of tramadol HCl from optimized nanoparticles was evaluated in phosphate phosphate buffered saline adjusted to a pH value of 7.4. The results are illustrated in (Fig. 4).As shown in the figure, the release profile indicated a slow and sustained release of tramadol from nanoparticles and 58.32±3.64%, 73.65±5.57% and 78.21±3.11% of the entrapped drug were released within 24 h, 48 h and 72 h post incubation, respectively. Similarly, various studies reported slow andprolonged release behavior of drugs encapsulated in SLNs [32-35]. In the study performed by Mueller et al. (2000), SLNs were suggested as the suitable carriers for prolonged drug release. In the study performed by Kushwaha et al. [35], the slow release of drug from solid lipid nanoparticles was justified by formation of increased diffusion barrier and the retarding

(cc) BY

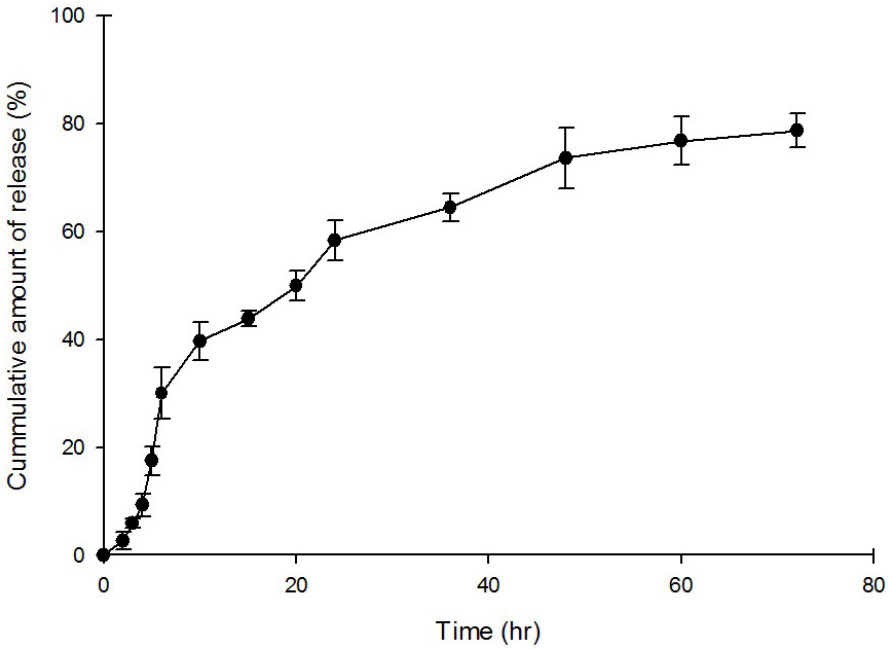

Fig. 4. Cumulative release profile of tramadol hydrochloride from SLN formulation (pH=7.4) (n=3);

Table 7. Parameters of drug release kinetics

Release Kinetic model	Equation	R^2	Adjusted R^2	Coefficients
Zero-order	$\frac{Mt}{M\infty} = K0.t$	0.6635	0.6633	K_0=0.0184
First -order	$\frac{Mt}{M\infty} = 1 - e^{(-k1t)}$	0.9781	0.9781	K_1=0.0547
Hixson-Crawel	$\sqrt[3]{m0} - \sqrt[3]{m} = Khc,t$	0.000	0.000	K_{hc}= 0.016
Higuchi	$\frac{Mt}{M\infty} = Kh.\sqrt{t}$	0.9345	0.9345	K_h=0.1295
Korsmeyer-Pepass	$\frac{Mt}{M\infty} = Kp,t^n$	0.9348	0.9249	K_p=0.1237 n=0.4281

effects of the lipid shells which does not allow surrounding aqueous medium to penetrate inside the particles and release the encapsulated through dissolution mechanism.

The obtained *in vitro* data were subjected to different mathematical kinetic models including zero order, first order, Higuchi, Hixon–Crowell and Korsmeyer-Pepas using Sigma-plot® software (version 10.0.0.54). As shown in (Table 7), release kinetic of optimized SLN formulation was best fitted to the first order as well as Korsmeyer-Peppas release kinetic models. In Korsmeyer-Peppas equation, n is the release exponent which determines if the release is a fickian diffusion (n <0.5), anomalous diffusion (0.5 < n < 1.0), case- II transport (n=1.0) and super case- II transport (n>1.0) in spherical drug delivery systems [36]. In this study, the release exponent was calculated as 0.4281 (Table 7) which describes fickian diffusion mechanism explained by first order release kinetic model. Similarly, in the studies performed by Priyankaand Hassan [37] and Kakkar et al. [38], first order kinetic was proposed for release of montelukast and curcumin from SLNs, respectively.

CONCLUSION

This study focuses on the preparation and *in vitro* characterization of SLNs containing tramadol HCl which were optimized by central-composite design. The effects of formulation variables including ratio of GMS/lecithin and the amount of drug on physico-chemical properties of nanoparticles were also studied. Optimized nanoparticles were characterized as smallest in

size and lowest in PdI while their zeta potential should fall in the range of -20 mV to -10 mV. Morphological study of nanoparticles revealed formation of non-aggregated, uniformly sized and spherical shaped particles bearing smooth surfaces. *In vitro* release studies were performed on optimized SLNs containing tramadol HCl and the results were showed sustained release profile of the therapeutic compound from nanoparticles up to 72 hours. The kinetic of release was assumed to be first-order.

Although, the obtained data suggest that solid lipid nanoparticles can be considered as an alternative way in preparation of a vehicle for transdermal delivery of tramadol hydrochloride as a hydrophilic compound and encapsulation of the drug in the inner aqueous phase can protect the therapeutic from environmental degradation, but stability of the structure of nanoparticles in pharmaceutical patches is yet to be studied. Moreover, from the clinical point- of- view and for higher efficacy in pain management, it is suggested that the final dosage form may incorporate both immediate release formulations (i.e. tramadol as free solution) accompanied by penetration enhancers for reduction of acute pains as well as the prolonged release solid lipid nanoparticles for management of chronic pains. Finally, incorporation of nanoparticles to pharmaceutical patches may alter the release rate of tramadol. Therefore the release profile from the final dosage form should be evaluated.

ACKNOWLEDGEMENT

This study was accomplished as the Pharm.D thesis of Mina Abbasnia This study was made possible by financial supports from deputy of research and technology, Hamadan University of Medical Sciences, Hamadan, Iran[GrantNo. 950228795].

CONFLICT OF INTERST

The authors report no conflict of interest.

REFERENCES

1. Leppert W, Łuczak J. The role of tramadol in cancer pain treatment—a review. Supportive Care in Cancer. 2004;13(1):5-17.
2. Malonne H, Coffiner M, Fontaine D, Sonet B, Sereno A, Peretz A, et al. Long-term tolerability of tramadol LP, a new once-daily formulation, in patients with osteoarthritis or low back pain. Journal of Clinical Pharmacy and Therapeutics. 2005;30(2):113-20.
[3] Olin BR. Central analgesics., In M. R. Riley (ed.), Drug Facts and Comparisons, 54th ed.Wolters Kluwer, St. Louis. 2000;817–818.
4. Nabi-Meibodi M, Vatanara A, Najafabadi AR, Rouini MR, Ramezani V, Gilani K, et al. The effective encapsulation of a hydrophobic lipid-insoluble drug in solid lipid nanoparticles using a modified double emulsion solvent evaporation method. Colloids and Surfaces B: Biointerfaces. 2013;112:408-14.
5. Rahman Z, Zidan AS, Khan MA. Non-destructive methods of characterization of risperidone solid lipid nanoparticles. European Journal of Pharmaceutics and Biopharmaceutics. 2010;76(1):127-37.
6. Vafaei SY, Dinarvand R, Esmaeili M, Mahjub R, Toliyat T. Controlled-release drug delivery system based on fluocinolone acetonide–cyclodextrin inclusion complex incorporated in multivesicular liposomes. Pharmaceutical Development and Technology. 2014;20(7):775-81.
7. Almeida AJ, Runge S, Müller RH. Peptide-loaded solid lipid nanoparticles (SLN): Influence of production parameters. International Journal of Pharmaceutics. 1997;149(2):255-65.
8. Mannam R, Yallamalli IM. Enhanced Both in vitro and in vivo Kinetics by SLNs Induced Transdermal System of Furosemide: A Novel Approach. Recent Patents on Drug Delivery & Formulation. 2018;11(3):187-97.
9. Priano L, Esposti D, Esposti R, Castagna G, De Medici C, Fraschini F, et al. Solid Lipid Nanoparticles Incorporating Melatonin as New Model for Sustained Oral and Transdermal Delivery Systems. Journal of Nanoscience and Nanotechnology. 2007;7(10):3596-601.
10. Dara T, Vatanara A, Nabi Meybodi M, Vakilinezhad MA, Malvajerd SS, Vakhshiteh F, et al. Erythropoietin-loaded solid lipid nanoparticles: Preparation, optimization, and in vivo evaluation. Colloids and Surfaces B: Biointerfaces. 2019;178:307-16.
11. Vakilinezhad MA, Tanha S, Montaseri H, Dinarvand R, Azadi A, Akbari Javar H. Application of Response Surface Method for Preparation, Optimization, and Characterization of Nicotinamide Loaded Solid Lipid Nanoparticles. Advanced Pharmaceutical Bulletin. 2018;8(2):245-56.
12. Espada R, Josa JM, Valdespina S, Dea MA, Ballesteros MP, Alunda JM, et al. HPLC assay for determination of amphotericin B in biological samples. Biomedical Chromatography. 2008;22(4):402-7.
13. Massella D, Leone F, Peila R, Barresi A, Ferri A. Functionalization of Cotton Fabrics with Polycaprolactone Nanoparticles for Transdermal Release of Melatonin. Journal of Functional Biomaterials. 2017;9(1):1.
14. Mahjub R, Radmehr M, Dorkoosh FA, Ostad SN, Rafiee-Tehrani M. Lyophilized insulin nanoparticles prepared from quaternizedN-aryl derivatives of chitosan as a new strategy for oral delivery of insulin:in vitro, ex vivoandin vivocharacterizations. Drug Development and Industrial Pharmacy. 2013;40(12):1645-59.
[15] ShahR, et al. Optimisation and stability assessment of solid lipid nanoparticles using particle size and zeta potential. Journal of Physical Sciences, 2014; 25(1):59-75.
16. Shah M, Pathak K. Development and Statistical Optimization of Solid Lipid Nanoparticles of Simvastatin by Using 23 Full-Factorial Design. AAPS PharmSciTech. 2010;11(2):489-96.
17. Mehnert W. Solid lipid nanoparticles Production, characterization and applications. Advanced Drug Delivery Reviews. 2001;47(2-3):165-96.
18. Trotta M, Debernardi F, Caputo O. Preparation of solid lipid

(cc) BY

nanoparticles by a solvent emulsification–diffusion technique. International Journal of Pharmaceutics. 2003;257(1-2):153-60.
19. Freitas C, Müller RH. Effect of light and temperature on zeta potential and physical stability in solid lipid nanoparticle (SLN™) dispersions. International Journal of Pharmaceutics. 1998;168(2):221-9.
[20] Malekpour MR, et al. Effect of various parameters on encapsulation efficiency of mPEG-PLGA nanoparticles: Artificial Neural Network. Biointerface research in applied chemistry, 2018; 8: 3267-3272.
21. Shahsavari S, Bagheri G, Mahjub R, Bagheri R, Radmehr M, Rafiee-Tehrani M, et al. Application of Artificial Neural Networks for Optimization of Preparation of Insulin Nanoparticles Composed of Quaternized Aromatic Derivatives of Chitosan. Drug Research. 2013;64(03):151-8.
22. Mahjub R, Heidari Shayesteh T, Radmehr M, Vafaei SY, Amini M, Dinarvand R, et al. Preparation and optimization of N-trimethyl-O-carboxymethyl chitosan nanoparticles for delivery of low-molecular-weight heparin. Pharmaceutical Development and Technology. 2014;21(1):14-25.
[23] Mueller RH, Maeder K, Gohla S. Solid lipid nanoparticles (SLN) for controlled drug delivery–a review of the state of the art. European Journal of Pharmaceutics and Biopharmaceutics, 2000; 50(1):161-177.
24. Severino P, Santana MHA, Souto EB. Optimizing SLN and NLC by 22 full factorial design: Effect of homogenization technique. Materials Science and Engineering: C. 2012;32(6):1375-9.
25. Schwarz C. Solid lipid nanoparticles (SLN) for controlled drug delivery II. drug incorporation and physicochemical characterization. Journal of Microencapsulation. 1999;16(2):205-13.
26. Zimmermann E, Müller RH, Mäder K. Influence of different parameters on reconstitution of lyophilized SLN. International Journal of Pharmaceutics. 2000;196(2):211-3.
27. Howard MD, Lu X, Jay M, Dziubla TD. Optimization of the lyophilization process for long-term stability of solid–lipid nanoparticles. Drug Development and Industrial Pharmacy. 2012;38(10):1270-9.
28. Abdelwahed W, Degobert G, Fessi H. A pilot study of freeze drying of poly(epsilon-caprolactone) nanocapsules stabilized by poly(vinyl alcohol): Formulation and process optimization. International Journal of Pharmaceutics. 2006;309(1-2):178-88.
29. Abdelwahed W, Degobert G, Stainmesse S, Fessi H. Freeze-drying of nanoparticles: Formulation, process and storage considerations. Advanced Drug Delivery Reviews. 2006;58(15):1688-713.
30. de Chasteigner Sp, Cav G, Fessi H, Devissaguet J-P, Puisieux F. Freeze-drying of itraconazole-loaded nanosphere suspensions: a feasibility study. Drug Development Research. 1996;38(2):116-24.
[31] Al-Qushawi A, et al. Preparation and characterization of three tilmicosin-loaded lipid nanoparticles: physicochemical properties and in-vitro antibacterial activities. Iranian Journal of Pharmaceutical Research, 2016; 15(4):663-676.
32. Venkateswarlu V, Manjunath K. Preparation, characterization and in vitro release kinetics of clozapine solid lipid nanoparticles. Journal of Controlled Release. 2004;95(3):627-38.
33. Vivek K, Reddy H, Murthy RSR. Investigations of the effect of the lipid matrix on drug entrapment, in vitro release, and physical stability of olanzapine-loaded solid lipid nanoparticles. AAPS PharmSciTech. 2007;8(4):16-24.
34. Daniher DI, Zhu J. Dry powder platform for pulmonary drug delivery. Particuology. 2008;6(4):225-38.
35. Kushwaha AK, Vuddanda PR, Karunanidhi P, Singh SK, Singh S. Development and Evaluation of Solid Lipid Nanoparticles of Raloxifene Hydrochloride for Enhanced Bioavailability. BioMed Research International. 2013;2013:1-9.
36. Ritger PL, Peppas NA. A simple equation for description of solute release I. Fickian and non-fickian release from non-swellable devices in the form of slabs, spheres, cylinders or discs. Journal of Controlled Release. 1987;5(1):23-36.
37. Priyanka K, Abdul Hasan SA. Preparation and Evaluation of Montelukast Sodium Loaded Solid Lipid Nanoparticles. Journal of Young Pharmacists. 2012;4(3):129-37.
38. Kakkar V, Singh S, Singla D, Kaur IP. Exploring solid lipid nanoparticles to enhance the oral bioavailability of curcumin. Molecular Nutrition & Food Research. 2010;55(3):495-503.

CC BY